Proceedings of the 17th
IEEE International Conference on Nanotechnology
Pittsburgh, USA, July 25-28, 2017

Tape-based Flexible Metallic and Dielectric Nanophotonic Devices and Metamaterials

Qiugu Wang, Weikun Han, Yifei Wang, Meng Lu, and Liang Dong
Department of Electrical and Computer Engineering
Iowa State University
Ames, IA, 50011, USA

Abstract—**This paper presents a multifunctional nanotransfer printing (nTP) method based on a simple stick-and-peel procedure that allows fast production of multiple optical nanodevices using Scotch tape. In addition to the capabilities of forming single- and multi-layer nanopatterned films on a tape, the present technique facilitates the transfer of nanostructures onto unconventional substrates (such as cleaved fiber facets and curved fiber sides) and fabrication of more complex optical devices, including Fabry-Perot cavities. Moreover, our stick-and-peel method can be applicable to various metallic and dielectric structures, including metamaterials with the feature size below 100 nm and TiO_2 nanopatterned films.**

Keywords—Nanopattern transfer; Tape; Plasmonics; Photonic crystal; Metamaterial

I. INTRODUCTION

Nanotransfer printing (nTP) is a cost-effective and high-throughput technology, which allows manufacturing of large-area nanopatterns.[1] This approach enables the transfer of functional nanopatterned metal or dielectric films from a stamp onto a variety of flexible or stretchable substrates for inexpensive thin-film transistors, integrated circuits, epidermal electronics, surface-enhanced Raman spectroscopy substrates, negative-index three-dimensional (3D) metamaterials, and microelectromechanical devices. Adhesive tapes, often used to exfoliate graphene or MoS_2 monolayers, have also been utilized in many nTP processes as intermediate transfer media or sacrificial layers. Because the adhesion strength of some functional adhesive materials can be varied using heat [2] or solvents [3], thermal adhesive tapes have been used for transferring nanotube transistors from quartz to plastic substrates, owing to the dramatic decrease in the tape adhesion strength at high temperatures. In addition, the presence of a thin adhesive polymer layer, whose adhesion strength can be controlled by using a plasticizing solvent, can promote high-fidelity replication and on-demand release of Au nanowires onto various supports. Apart from functioning as sacrificial layers, adhesive tapes have also been utilized for planarizing nanopatterned substrates to generate large-area nanogaps, [4] and serving as a substrate for the transfer of Al nanohole films from compact discs under a critical temperature [5].

In this work, we present a Scotch tape based nTP process that enables easy transfer of nanopatterned films and cost-effective manufacture of multiple optical nanodevices. Noble metals such as Au and Ag are suitable materials for implementing tape-based nTP process because of the poor adhesion to polydimethylsiloxane (PDMS) or Si. This feature, combined with simple replica nanomolding process using PDMS or Si stamps, makes it possible to build large-area, low-cost and ready-to-use optical devices on flexible tapes.

As illustrated in Fig. 1a, the method of direct tape pasting (stick and peel-off) of nanohole films from PDMS stamps forms the basis of other processes. This simple procedure also applies to multi-layer metal-dielectric-metal (MIM) and all-dielectric films as well as metamaterials from Si wafers. In addition, solvents-assisted transfer of Au nanohole films onto optical fibers are presented. In particular, the described taping method also allows fast and more cost-effective generation of advanced optical devices, such as the tape-supported Fabry-Perot (FP) cavities. The resulting tape-supported nanostructures can retain excellent electrical and optical performance, which can be potentially useful for disposable electronic and optical sensors as well as in ready-to-use microscopic applications.

II. METHODS

A. Fabrication of PDMS stamps

During fabrication of PDMS stamps, a soft lithography-based replica molding process [6-8] has been utilized to produce a polymer nanopost array from PDMS elastomer. In this step, a Si template (LightSmyth Technologies Inc., OR, USA) is used as a solid master mold, which is composed of 9 patterns with areas of 8 mm × 8 mm. The Si mold exhibits the following three pattern types: 1D grating, 2D nanopost arrays, and 2D nanohole arrays. In contrast to the patterns observed for the Si mold, PDMS stamps obtained after replica molding exhibit the inverse structures.

B. Fabrication of complementary metamaterials

The complementary metamaterial has been fabricated on a SOI wafer. First, the top Si layer of the SOI substrate is thinned down to around 20 nm by thermal oxidation with subsequent wet etching. After that, U-shaped air gaps are patterned on the thinned Si layer surface via e-beam lithography and subsequent reactive-ion etching. The resulting wafer is immersed into a buffered oxide etch solution for 5 min to remove the SiO_2 layer underneath the top Si membrane, while retaining most of the SiO_2 film underneath the frame structure between neighboring c-SRRs. Consequently, the Si c-SRR membrane is suspended above the air cavities. Finally, a 40 nm thick Au film is evaporated onto the device surface to form Au/Si c-SRRs on the top and Au solid SRRs on the bottom of the air wells.

C. Electron beam evaporation

An electron beam evaporator Temescal (BJD–1800) has been used to deposit single-layer multilayer films with thicknesses of 40 nm onto the stamp surface at an average chamber pressure of around 1×10^{-6} Torr and deposition rate of around 1 Å/s. No additional layers are deposited between the Au and SiO_2 components.

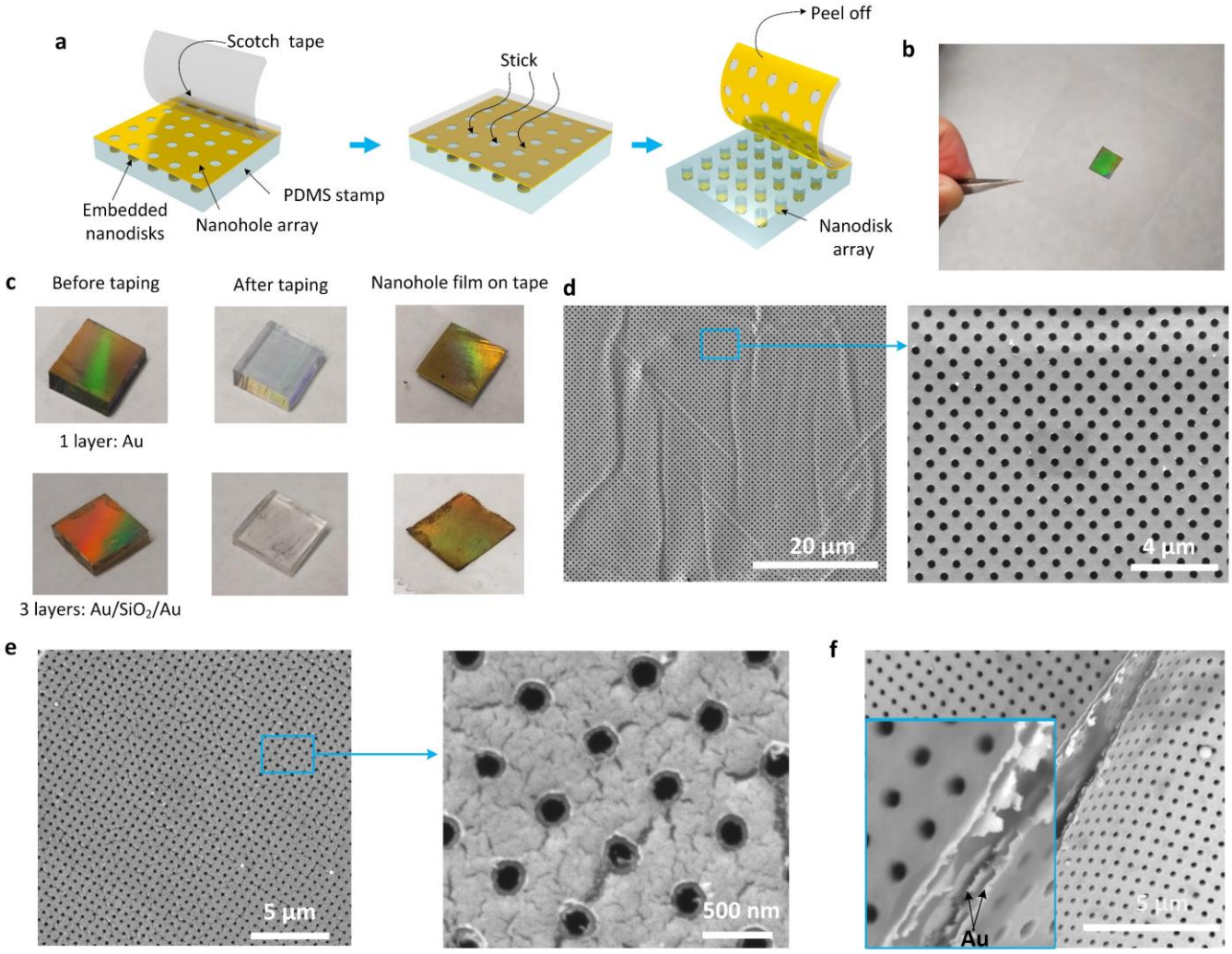

Fig. 1 Stick-and-peel taping method of producing Au nanopatterned films on the Scotch tape surface. a, A schematic illustration of the taping procedure utilized for stripping the Au nanohole array from the Au-coated PDMS stamp containing periodic nanowells with depths of 350 nm. **b**, A photograph of the stripped Au nanohole array on the tape substrate. The area of the Au film is approximately 8 × 8 mm^2. **c**, Photographs of the 1-layer Au and 3-layer Au/SiO_2/Au films on the PDMS stamp before (left panel) and after (middle panel) taping. The right panel shows the nanohole arrays transferred onto the tape surface. **d**, SEM images of the stripped single-layer Au nanohole array on the tape surface. **e**, SEM images of the stripped Au/SiO_2/Au films on the tape surface. **f**, A cross-sectional view of the 3-layer Au/SiO_2/Au film. The inset shows the magnified cross-sectional image containing the top and bottom Au layers. The nanohole arrays depicted in panels **d–f** have a period of 600 nm and are arranged in a square pattern.

D. Optical measurements and simulations

Optical spectra of the nanohole arrays on the tape surface or nanodisks embedded into the PDMS layer have been recorded using a spectroscopic measurement setup. The white light emitted from a 150 W quartz halogen lamp is coupled into a multimode fiber collimated by an objective lens and directed onto the sample surface. Reflection spectra of the complementary metamaterials on the tape surface are recorded via Fourier transform infrared spectroscopy (Hyperion 2000, Bruker) under normal incidence of light. Optical simulations have been performed using the finite element method of the COMSOL Multiphysics commercial software [9]. The geometrical parameters used in the simulations are obtained from the SEM images of the studied samples.

III. Results and Discussion

A. Stick-and-peel taping procedure

Fig. 1a schematically illustrates the taping procedure consisting of sticking and peeling off Au films patterned with nanohole arrays from a PDMS nanostamp. PDMS stamps containing periodic nanowells are generally fabricated from a Si master using a soft lithography-based replica molding process (see the Methods section). After depositing a 40 nm thick Au layer onto a PDMS stamp, quasi-3D plasmonic crystals containing Au nanohole arrays at the top and PDMS-embedded nanodisks are formed. General-purpose transparent pressure-sensitive adhesive tape (Scotch® Shipping packaging, 3M, MN, USA) is used for peeling off Au nanopatterned films. The tape with a total thickness of 79 µm is composed of 51 µm thick biaxially oriented polypropylene backing and 28 µm thick adhesive fabricated from hot-melt rubber resin. At 23°C, a tape piece with dimensions of around 40 × 40 mm^2 is directly applied to the surface of the Au-coated PDMS stamp and smoothed down with fingertips. Due to the poor adhesion strength between Au and PDMS, the Au nanopatterned films can be easily peeled off from the substrate surface (see inset in Fig. 1a), while the nanodisks remain embedded into the PDMS bulk. The scanning electron microscopy (SEM) images of the Au nanohole arrays on the tape surface depicted in Fig. 1c exhibit excellent uniformity over large areas despite the presence of micrometer-scale wrinkles.

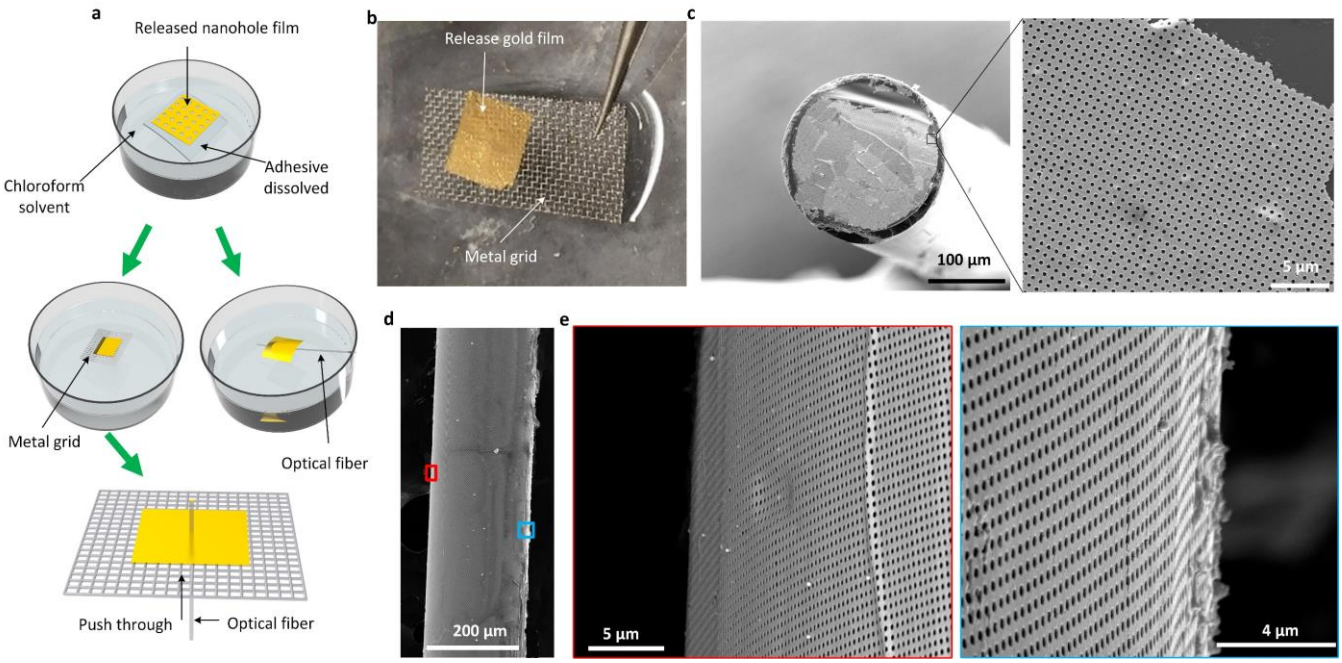

Fig. 2 Solvent-assisted transfer of Au nanohole arrays from the adhesive tape onto the optical fiber surface. a, A schematic of the release-and-transfer process of Au nanohole arrays onto the optical fiber surface. Chloroform solution is used to remove adhesives from the tape. The Au nanohole arrays can be transferred onto the fiber tip with a diameter of 210 μm by pushing the fibers through the holes in the metal grid (with dimensions of 500 × 500 μm^2) covered with Au nanohole arrays. Alternatively, the Au nanohole arrays can be directly accommodated by an optical fiber to form a curved nanohole film on its surface. **b**, Photographs of the released Au nanohole array and metal grid substrate. **c**, SEM images of the Au nanohole array deposited on the fiber facet. **d**, SEM images of the curved Au nanohole array on the fiber surface.

To further investigate the ability of the proposed taping method to form multilayers of nanohole arrays, the utilized PDMS stamp has been covered with alternating layers of Au and SiO_2. In our experiment, a 5-layer film (Au/SiO_2/Au/SiO_2/Au; 40 nm thick each) is deposited onto the PDMS nanowell arrays without enhancing the adhesion between the Au and SiO_2 layers. As shown in Fig. 1b, the 1-layer and 3-layer films are mostly peeled off from the PDMS substrate. The maximum number of layers that can be peeled off from the tape surface can be determined by the poor bonding strength between the Au and SiO_2. The 3-layer alternating metal/dielectric film transferred onto the tape surface also exhibits high uniformity, as can be illustrated by Fig. 1d, although its quality is not as good as that of the 1-layer Au film. It should be noted that other types of PDMS stamps as well as 2D periodic nanopost arrays can be used in the taping procedure. However, because the applied mechanical pressure deforms PDMS nanoposts during sticking, some nanodisks are also transferred along with metal films from the bottom of the PDMS stamp to the tape surface.

B. Solvent-assisted transfer process

One notable advantage of the proposed taping method is that it allows convenient transfer of Au nanopatterned films from the tape surface onto various substrates, which can be realized by wet etching of the tape adhesive with chloroform solvent. In this study, Au nanohole arrays are transferred onto the cleaved facet and curved side of an optical fiber, as schematically illustrated in Fig. 2a. First, the tape containing Au nanohole surface arrays is fully immersed into chloroform until the Au film is completely detached from the tape. The time required for the delamination of the Au film depends on the number of the deposited layers and is equal to 40 s for the single-layer Au film and 2 min for the 3-layer Au/SiO_2/Au film. Afterwards, the suspended Au film is picked by the metal grid with a hole size of 500 × 500 μm^2, as shown in Fig. 2b. Before the chloroform layer on the metal grid surface completely dries out (in less than 20 s), an optical fiber is directly pushed through the hole covered with the nanopatterned film from the grid downside. As a result, the part of the Au nanopatterned film that is in contact with the fiber tip is transferred onto the fiber surface. Fig. 2c shows the SEM image of the transferred Au nanohole arrays on the cleaved fiber facet containing a large area of the uniform nanopatterned film.

The majority of the existing patterning techniques directly produce nanopatterns on the fiber facet using lithographical or self-assembly methods, which are expensive or difficult to operate. Nanoskiving [10] is a convenient technique for manually transferring nanopatterns onto the fiber facet using an immersion procedure, the key part of which corresponds to sectioning nanostructures embedded in thin epoxy slabs and is time-consuming. In contrast, the proposed taping method of transferring nanopatterned films is relatively simple and fast. However, while the nanoskiving method uses epoxy slabs for supporting nanostructures, the nanopatterned films fabricated in this work are attached to freestanding metal grids; as a result, the surface tension produced by the chloroform evaporation causes the breakage and stacking of the Au films in some random areas with a yield of around 50%. Thus, the quality of the transferred nanopatterns is slightly lower than that obtained by the nanoskiving method. To reduce surface tension, Au films can be immersed into an ethanol solution immediately after the removal from the chloroform etching solution. Interestingly, after the complete ethanol evaporation, freestanding Au nanohole films with areas of tens of μm^2 supported by the metal grid can be obtained. Another minor problem of the described transfer method is the breakage of fiber edges during pushing through the metal grid holes (Fig. 2c). Alternatively, the direct lift-up of the Au nanopatterned film

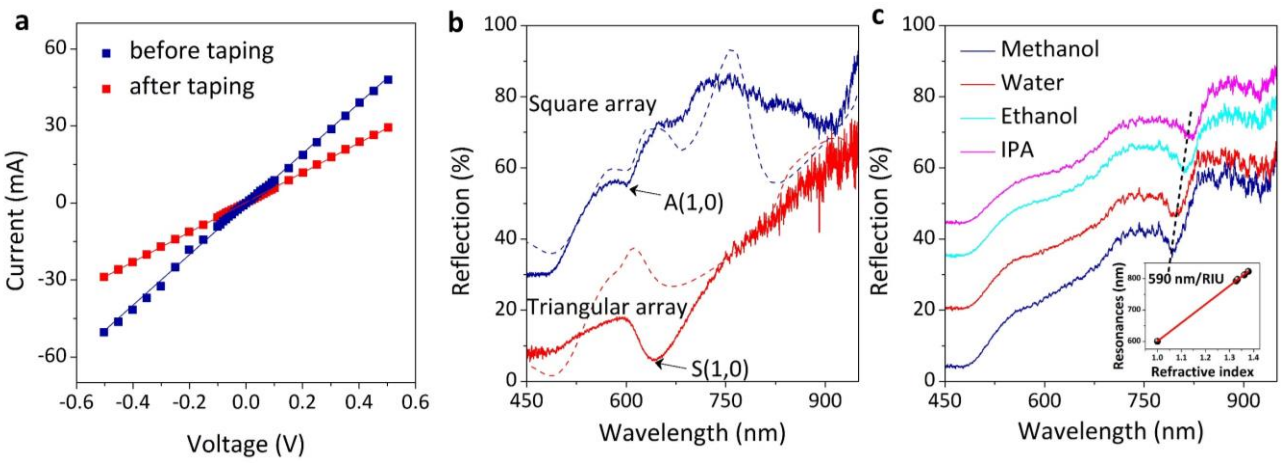

Fig. 3 Electrical and optical performance of the Au nanohole arrays on the tape surface. a, I–V curves recorded for the nanopatterned Au film before and after taping. **b**, Experimental (solid lines) and simulated (dash lines) reflection spectra obtained for the Au nanohole arrays on the tape surface. Both nanohole arrays have a period of 600 nm and are arranged in square and hexagonal patterns. A(1,0) and S(1,0) denote the (1,0) SPP excitations at the air/Au and tape/Au interfaces, respectively. **c**, Bulk refractive index sensitivities measured for the tape-supported square Au nanohole arrays with a period of 600 nm. The inset shows the linear fit of the resonance wavelength plotted as a function of the refractive index.

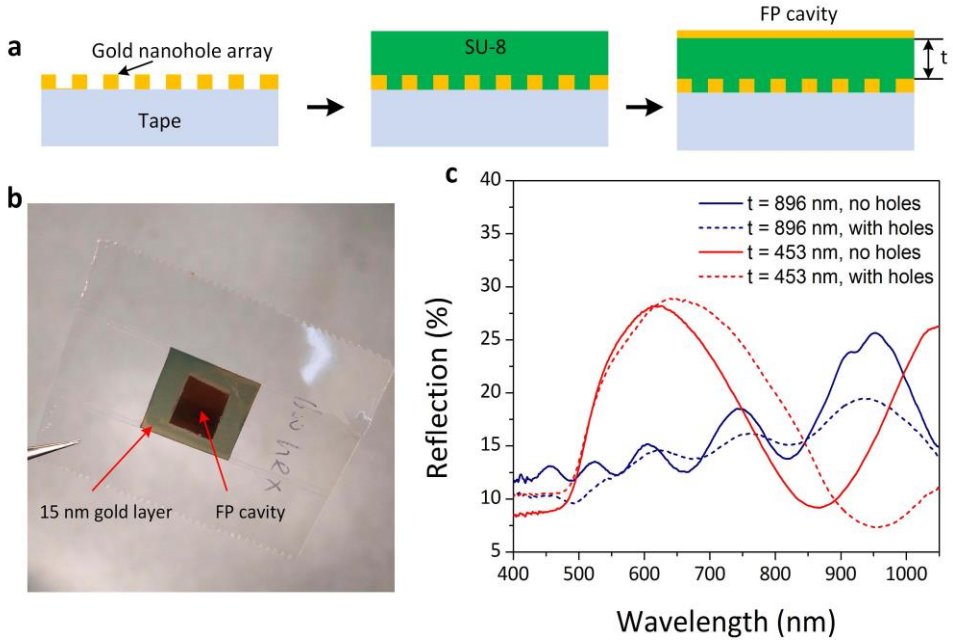

Fig. 4 Fabry-Perot cavities formed on the tape surface. a, Fabrication of FP cavities. After transferring Au nanoholes or plain films on the Scotch tape surface, it has been spin-coated with a SU–8 photoresist layer with a thickness *t* followed by the deposition of a 15 nm thick Au layer. **b**, Reflection spectra recorded for the FP cavities on the tape surface with and without nanoholes under normal light incidence. The studied Au nanohole array is arranged into a hexagonal pattern with a period of 600 nm.

supported on the fiber surface enables its attachment to the curved fiber sides. In contrast to the former process of transferring nanopatterns on the fiber facets (without intermediate attachment to a metal grid), this process allows more uniform formation of nanopatterns on the curved fiber side, as shown in Figs. 2d and e.

C. Electrial and optical characterizations

a) Electrical and refractive index sensitivity measurement

Figures 3a–c describe the electrical and optical properties of the Au nanohole arrays on the Scotch tape surface. After their transfer, the arrays still exhibit high conductivity with a 40% decrease from 0.1 S to 0.06 S (see Fig. 3a). Figure 3b shows the experimental and simulated reflection spectra obtained for the tape-supported square and triangular spaced nanohole arrays with periods of 600 nm. The optical resonances of these two arrays correspond to the reflectance dips detected at 600 nm and 637 nm. As indicated by the simulations, the two resonances denoted as A(1,0) and S(1,0) in Fig. 3b are due to the (1,0) SPP excitations observed at the air/Au and tape/Au interfaces for the square and triangular spaced nanohole arrays, respectively. The bulk index sensitivity measured for the A(1,0) resonance of

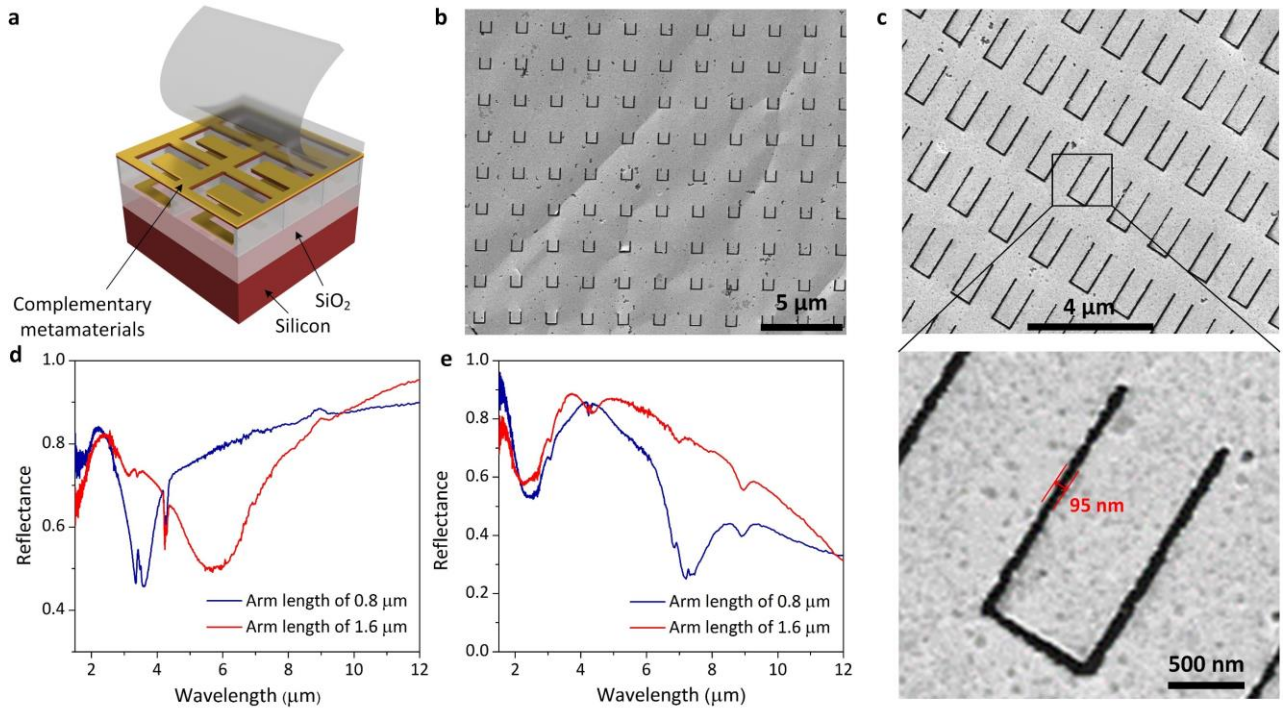

Fig. 5 Taping method applied to quasi-3D metamaterials and dielectric nanopatterned films. a, Schematic of a quasi-3D metamaterial. **b**,**c**, SEM images of the tape-supported Au complementary metamaterials. The U-shape of the air apertures of both devices has a width of 500 nm, and 100 nm wide air gaps are arranged in a rectangular pattern. The device depicted in panel (**b**) possesses an arm length of 800 nm and period of 1.6 µm in both directions, while the device depicted in panel (**c**) has a 1.6 µm long arm and periods of 1.6 µm and 2.6 µm in two orthogonal directions. **d**,**e**, Reflection spectra recorded for two Au complementary metamaterials.

the square nanohole array is equal to 590 nm/RIU (see Fig. 3c), indicating excellent index sensing capabilities of the transferred arrays.

b) Fabry-Perot cavities on the tape surface

In this section, more complex optical structures based on the transferred Au nanohole films such as Fabry-Perot (FP) cavities on the tape surface have been investigated (their fabrication procedure is illustrated in Fig. 4a). First, a SU−8 photoresist layer with a certain thickness is spin-coated onto the surface of the tape-supported Au nanohole film followed by the deposition of a 15 nm thick Au layer. Figure 4b shows the reflection spectra recorded for the devices with cavity lengths of 896 and 453 nm. For comparison purposes, the devices containing plain Au films (without nanohole arrays) have been fabricated as well. At a cavity length of 896 nm, the predicted second-order FP mode (which is estimated using the reflection coefficients derived in Ref. [11]) corresponds to a wavelength of 1550 nm, and higher orders of the FP resonance are also observed in the measured wavelength range. However, for the devices with a cavity length of 453 nm, the second-order FP mode is calculated at a wavelength of 850 nm, which agrees well with the observed dip at 860 nm depicted in Fig. 4b. Hence, the devices containing nanohole arrays exhibit optical properties similar to those of the systems without nanohole arrays (with a slight redshift of all FP modes).

D. Metasurface and dielectric nanohole films on the tape

In addition to peeling off Au films from PDMS stamps, the described taping method can also be applied to stamps made of other materials or dielectric nanopatterned films supported by PDMS stamps. In this work, the following two examples are discussed: quasi-3D metamaterials on silicon-on-insulator (SOI) wafers (Fig. 5a) and TiO_2 nanohole arrays on PDMS stamps (Fig. 6a). The utilized quasi-3D metamaterial is composed of an array of Au−Si bilayer complementary split ring resonators (c-SRRs) at the top and an array of Au SRRs at the bottom of the wells with depths of several hundred nanometers formed inside a 1 µm thick SiO_2 layer of the SOI substrate. Each c-SRR unit has an Au−Si nanocantilever surrounded by a U-shaped air gap. After the taping procedure, the top Au c-SRR arrays are transferred onto the tape surface, as shown in Figs. 5b and c. The feature size of the air gap of c-SRRs is around 95 nm. The reflection spectra obtained for the c-SRR arrays depicted in Figs. 5d and f exhibit conspicuous resonance dips, which are associated with the excitations of even or odd c-SRR eigenmodes by transverse-magnetic (TM)- or transverse-electric (TE)-polarized fields. For example, under TM polarization, the second order c-SRR excitation mode of the device with an arm length of the U-shape air apertures of 1.6 µm is observed at 6 µm, while the device with a 0.8 µm long arm exhibits the second order c-SRR excitation mode

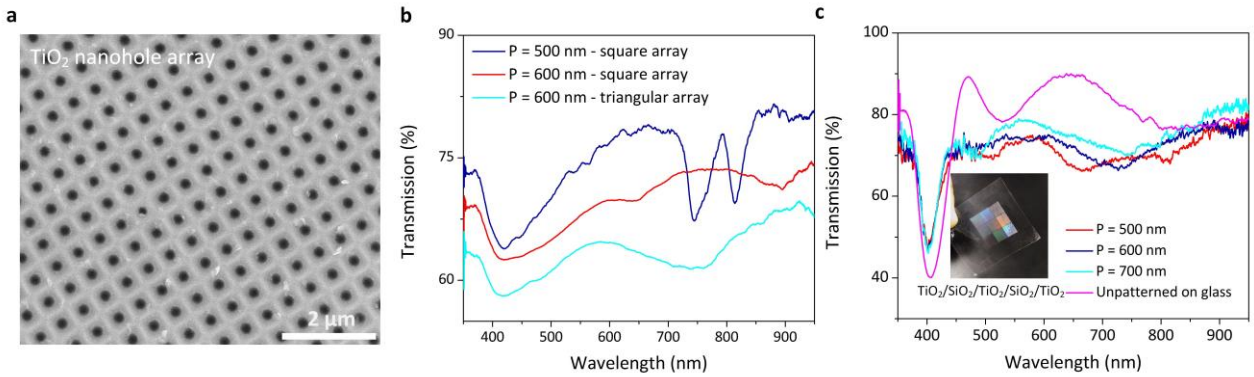

Fig. 6. a, An SEM image of the single-layer TiO_2 nanohole array transferred onto the tape surface. **b**, Transmission spectra recorded for the TiO_2 nanohole arrays with different periods arranged in square and triangular patterns. **c,** Photographs of the 5-layer $TiO_2/SiO_2/TiO_2/SiO_2/TiO_2$ nanohole film on the tape surface. **d**, Transmission spectra recorded for the transferred 5-layer $TiO_2/SiO_2/TiO_2/SiO_2/TiO_2$ film with different periods and 5-layer film directly deposited on the glass slide. The transmission dip observed at 400 nm clearly indicates thin-film destructive interference.

at 3.8 μm. Therefore, this infrared metasurface could be used for sensing of infrared radiation [12].

The TiO_2 nanohole arrays shown in Fig. 6a exhibit high uniformity, and their transmission spectra contain resonance features depending on the array period. In contrast to peeling off alternating metal and dielectric films, all-dielectric 5-layer $TiO_2/SiO_2/TiO_2/SiO_2/TiO_2$ films with enhanced bonding strengths between TiO_2 and SiO_2 can be easily removed from PDMS stamps. This stack of alternating index-contrast materials demonstrates clear thin-film destructive interference at a wavelength of 400 nm (see the transmission spectra depicted in Fig. 6c), confirming the complete transfer of the 5-layer film onto the tape surface.

IV. Conclusions

In summary, a series of nanotransfer processes utilizing general adhesive tapes have been successfully demonstrated. Using a straightforward stick-and-peel method, both the 3-layer $Au/SiO_2/Au$ and 5-layer $TiO_2/SiO_2/TiO_2/SiO_2/TiO_2$ nanohole films can be directly transferred from PDMS stamps onto the adhesive tape surfaces. In addition to the realization of metasurface and many other nanophotonic devices, it is also our interest to integrate this technology to realize tape-based optical and optofluidics based biochemical sensing [13, 14]

Acknowledgment

This work was supported by the U.S. National Science Foundation under Grant # ECCS-0954765. The authors also thank Shawana Tabassum for providing some molds and Seval Oren for discussion on peeling process.

References

[1] A. Carlson, A. M. Bowen, Y. Huang, R. G. Nuzzo, and J. A. Rogers, "Transfer printing techniques for materials assembly and micro/nanodevice fabrication," Adv. Mater., vol. 24, pp. 5284–5318, August 2012.

[2] C. H. Lee, D. R. Kim, and X. Zheng, "Fabricating nanowire devices on diverse substrates by simple transfer-printing methods," Proc. Natl. Acad. Sci., vol. 107, pp. 9950–9955, June 2010.

[3] J. W. Jeong, *et al,* "High-resolution nanotransfer printing applicable to diverse surfaces via interface-targeted adhesion switching," Nat. Commun., vol. 5, pp. 5387, November 2014.

[4] X. Chen, *et al,* "Atomic layer lithography of wafer-scale nanogap arrays for extreme confinement of electromagnetic waves," Nat. Commun., vol. 4, pp. 2361, September 2013.

[5] C. A. Barrios, and V. Canalejas-Tejero, "Compact discs as versatile cost-effective substrates for releasable nanopatterned aluminium films," Nanoscale, vol. 7, pp. 3435–3439, January 2015.

[6] Q. Wang, W. Han, P. Liu, and L. Dong, "Electrically tunable quasi-3D mushroom plasmonic crystal," J. Lightwave Technol., vol. 34, pp. 2175-2181, May 2015.

[7] P. Liu, *et al*, "Tunable meta-atom using liquid metal embedded in strectcable polymer," J. App. Phys., vol. 118, pp. 014504, July 2015.

[8] S. Yang, *et al*, "From flexible and strectchable meta-atom to metamaterial: A wearable microwave meta-skin with tunable frequency selective and cloaking effects," Sci. Rep., vol. 6, pp. 21921, February 2016.

[9] Q. Wang, *et al*, "Tunable optical nanoantennas incorporating bowtie nanoantenna arrays with stimuli-responsive polymer," Sci. Rep., vol. 5, pp. 18567, December 2015.

[10] D. J. Lipomi, *et al,* "Patterning the tips of optical fibers with metallic nanostructures using nanoskiving," Nano Lett., vol. 11, pp. 632–636, December 2010.

[11] C. P. Huang, *et al,* "Deep subwavelength Fabry-Perot-like resonances in a sandwiched reflection grating," Phys. Rev. B, vol. 85, pp. 235410, June 2012.

[12] L. Dong, R. Yue, L. Liu, and S. Xia, "Design and fabrication of single-chip a-Si TFT-based uncooled infrared sensors," Sens. Actuators, A, vol. 116, pp. 257-263, June 2004.

[13] L. Dong and H. Jiang, "Selective formation and removal of liquid microlenses at predetermined locations within microfluidics through pneumatic control," J. Microelectromech. Syst,. vol. 17, pp. 381-392, August, 2008.

[14] H. Yang and L. Dong, "Selective nanofiber deposition using a microfluidic confinement approach," Langmuir, vol. 26, pp. 1539-1543, December, 2009